



**Acoustics'08
Paris**
June 29-July 4, 2008

www.acoustics08-paris.org

Reduced Scale Experiment of Frequency Dependence of Single Spherical Biconcave Acoustic Lens for Ambient Noise Imaging

Kazuyoshi Mori, Hanako Ogasawara and Toshiaki Nakamura

National Defense Academy, 1-10-20 Hashirimizu, 239-8686 Yokosuka, Japan
kmori@nda.ac.jp

Based on numerical analysis using the Finite Difference Time Domain method and the reduced scale experiment of one-fifth space in our previous studies, we predicted that the spherical biconcave lens with an aperture diameter of 2.0 m would have sufficient directional resolution (for example, the beam width is 1 deg at 60 kHz) to realize the Ambient Noise Imaging (ANI) system. In this study, to confirm the directional resolution of the lens in a wide frequency band of 20-100 kHz, we performed a reduced scale experiment of one-fifth space in a water tank again. The lens, made of acrylic resin, has an aperture diameter of 400 mm and a radius of curvature of 500 mm. Burst pulses at 100, 200, 300, and 500 kHz, in which the frequency increases 5 times, were radiated from the sound sources to the lens. The lens with an aperture diameter of 2.0 m has fine directional resolution over 60 kHz in the original scale, because the main-lobe at 500 kHz was narrower than that at 300 kHz in the beam pattern of the reduced scale experiment.

1 Introduction

Ocean ambient noise distorts the sound characteristics of target signals; thus, it hinders target detection in a conventional sonar system. However, ambient noise is viewed as a sound source rather than a hindrance in a new concept called Ambient Noise Imaging (ANI). This is the third sonar method that is neither passive nor active to use natural sound in the ocean [1]. Some realistic systems have been built for ANI. The Acoustic Daylight Ocean Noise Imaging System (ADONIS), consisting of a spherical reflector 3 m in diameter, faced with closed-cell neoprene foam and having an array of 126 piezoelectric ceramic hydrophones attached to the focal surface, was built by Epifanio *et al.* as a first-generation ANI system. Using this system, silent target objects were successfully imaged against the ocean natural background noise, which was mainly generated by snapping shrimp [2]. Recently, the Remotely Operated Mobile Ambient Noise Imaging System (ROMANIS), consisting of a two-dimensional (2-D) sparse array of 504 hydrophones fully populating a 1.44 m circular aperture, was built by Venugopalan *et al.* as a second-generation system. They also successfully detected target objects using snapping shrimp noises in the warm shallow waters around Singapore [3].

On the other hand, an acoustic lens is a powerful choice for realizing an ANI system because it does not require a large receiver array and a complex signal processing unit for 2-D beam forming; thus, system minimization is facilitated and costs will be reduced. The analysis of a sound field focused by an acoustic lens is indispensable for designing imaging sonar systems. In our past studies, we analyzed a sound pressure field focused by an acoustic lens system constructed for an ANI system with a single spherical biconcave lens using the finite difference time domain (FDTD) method. Our aim was the development of a lens with a directional resolution similar to the beam width of ROMANIS, which is 1 deg at the frequency of 60 kHz. In an analysis using a 2-D or three-dimensional (3-D) FDTD method, the aperture diameter of 2.0 m with a sufficient resolution was roughly determined by comparing the image points and -3 dB areas of the sound pressure fields obtained using lenses with various apertures [4, 5].

It is also indispensable to confirm the numerical analysis results using a 3-D FDTD method by measuring the sound pressure field focused by a real lens. However, we wanted to avoid paying a high cost to make a huge lens of 2.0 m diameter at an early stage of designing the ANI system. By working at a reduced scale, we lowered the risk of a costly

failure because the smaller lens could be manufactured at a low cost. In our previous study, we performed a reduced scale experiment to lower the scale to one-fifth the original size of the lens in a water tank. The lens, made of acrylic resin, also has an aperture diameter and a radius of curvature that are one-fifth the original values under the numerical analysis condition. A burst pulse of 300 kHz was radiated from the sound source toward the lens. Thus, the frequency was five times larger than the target center frequency of 60 kHz on the original scale. The sound pressure after passage through the acoustic lens was measured by moving the receiver around the image point. We then compared the experimental results for the sound pressure distributions and -3 dB areas with the numerical analysis results at small incidence angles. We verified that this lens has a sufficient directional resolution from the observation indicating that -3 dB areas do not overlap each other at each incidence angle in the experimental results [6, 7].

The dominant noise sources for ANI are mainly generated by snapping shrimps in the coastal water. Because those noises have a wide frequency band [8], it is also indispensable to confirm the frequency dependence of the convergence characteristics of the acoustic lens. In this study, to confirm the directional resolution of the lens in a wide frequency band of 20-100 kHz, we performed a reduced scale experiment of one-fifth space in a water tank again. The lens, like that used in the previous study, has an aperture diameter of 400 mm and a radius of curvature of 500 mm. Burst pulses at 100, 200, 300, and 500 kHz were radiated from the sound sources to the lens. We compared the experimental results of the on-axis characteristics and beam patterns with those of the numerical analysis results using the 3-D FDTD method.

2 Conditions of Numerical Analysis

The arrangement for the 3-D FDTD method [9-11] is shown in Fig. 1. Figure 1(a) shows the analysis domain of the x - z plane ($y=0$) bounded by the absorption layer (shown here in gray). The y - z plane and x - y plane are shown in Fig. 1(b) and Fig. 1(c), respectively. To reduce the calculation volume, we halved the analysis domain on the y -axis using the symmetric condition with respect to the x - z plane at $y=0$. The lens, made of acrylic resin, has an aperture of 2.0 m and a radius of curvature of 2.5 m. The center of the lens is 0.05 m thick. The plane source (dotted line) is 0.55 m from the lens center. A Gaussian-windowed sin wave at 20, 40, 60, and 100 kHz is radiated from the plane source. The incidence angle θ is from 0 to 2 deg. The sound speeds and the densities are 1500 m/s and 1000 kg/m³, respectively, in

water and in the absorption layer, and 2670 m/s and 1200 kg/m³, respectively, in the lens. The attenuation constant of water is 0.0 dB/λ, since the attenuation in water is neglected. In the lens, the attenuation constant is 1.0 dB/λ, and it is 5.0 dB/λ in the absorption layer. Mur's first-order absorbing boundaries are applied to the exteriors to eliminate the reflection wave from the outer boundary of the analysis domain. The increments are 2.5 mm of space and 0.5 μs of time at the frequencies of 20, 40, and 60 kHz, and 1.5 mm and 0.3 μs at 100 kHz.

The examples of relative pressure distributions are shown in Fig. 2. The colors of these figures indicate the relative pressure at which the sum of the squared sound pressure at all time steps is normalized by the maximum value; the results for the x-z plane at y=0 have been extracted. There are prominent peaks at z=2.5 m. The figures show that the distribution centered at each focal point becomes sharp in proportion to the increase of frequency.

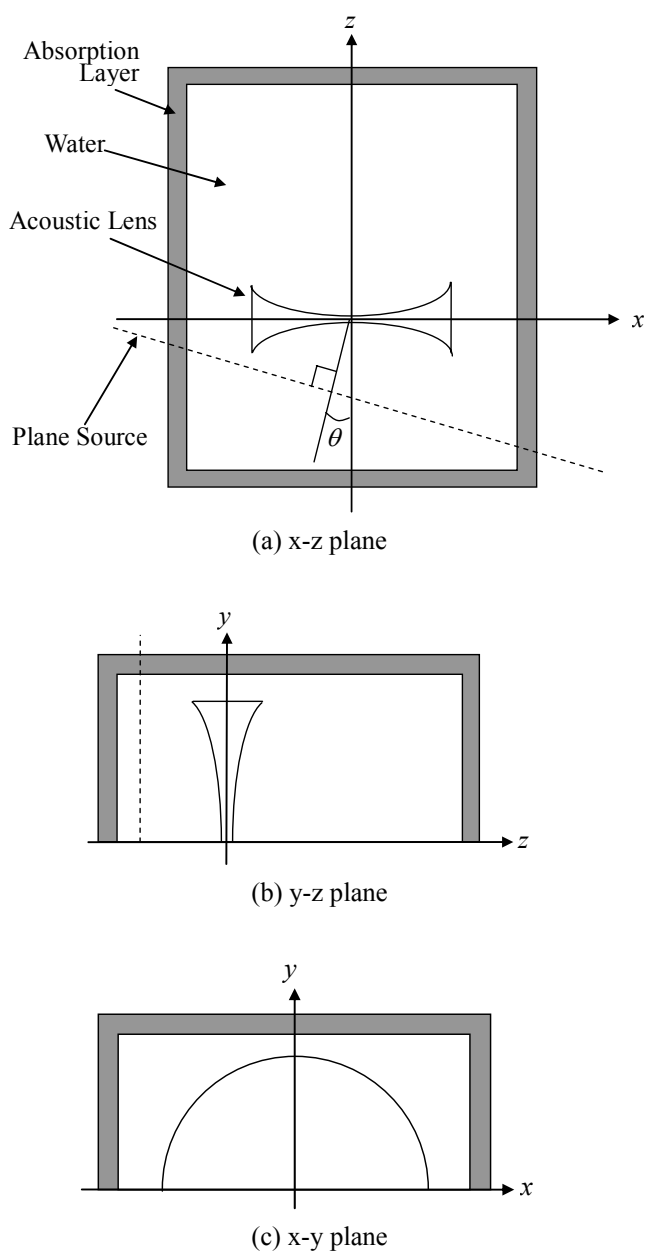


Fig. 1 Analysis domain of the 3-D FDTD method.

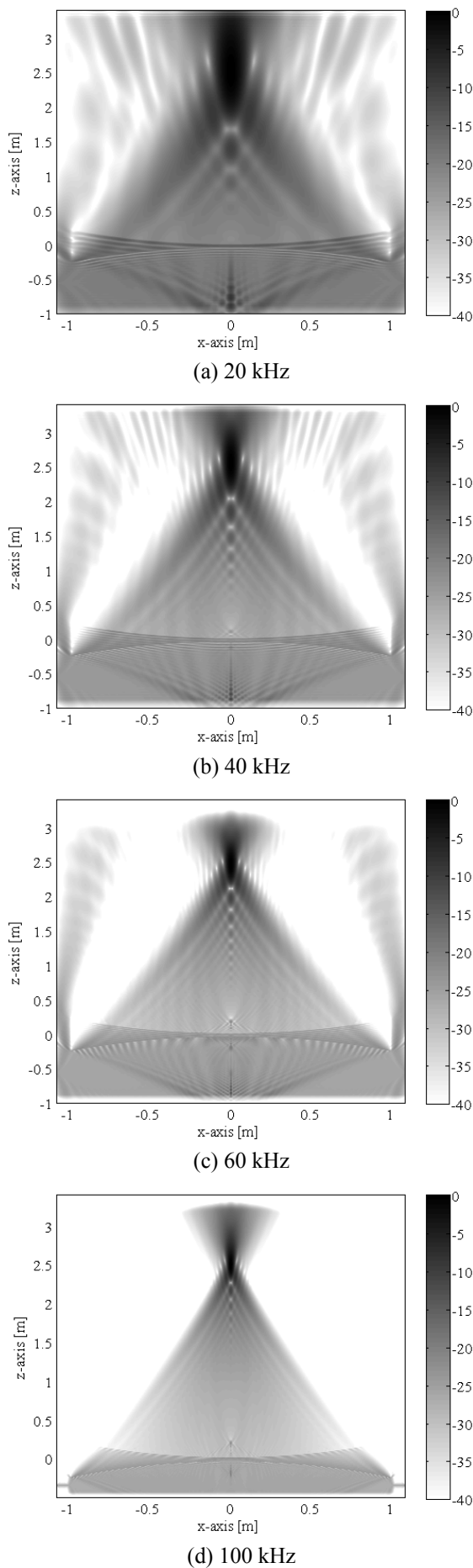


Fig. 2 Relative sound pressure distribution on the x-z plane at y=0 obtained by the 3-D FDTD method at normal incidence.

3 Experimental Setup

The experimental arrangement of the sound source, the receiver, and the acoustic lens in the water tank is shown in Fig. 3. The water tank is 7 m wide, 9 m long, and 5 m deep. The distance between the sound source and the center of the acoustic lens is 7 m. Burst pulses at 100, 200, 300, and 500 kHz were radiated from the sound sources. Here, the frequency is five times that obtained by numerical analysis. The sound pressure after passage through the acoustic lens was measured by moving the receiver. The diameter of the receiver is 4 mm, and the receiver has a flat frequency response up to 800 kHz. The x-y-z stage controls the position of the receiver within an accuracy of ± 0.01 mm. The acoustic lens arranged perpendicular to the z-axis is a spherical biconcave lens with an aperture diameter of 400 mm, a radius of curvature of 500 mm on each side, and a center thickness of 10 mm. These values are one-fifth those used in the numerical analysis.

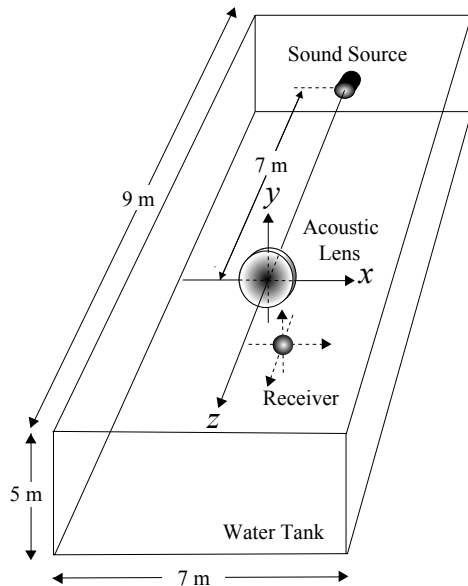


Fig. 3 Experimental Setup.

4 Results

4.1 Resolution at the target center frequency

The relative pressure distributions around the image point on the x-z plane at $y=0$ are compared in Fig. 4. The frequency is 300 kHz, which is the target center frequency on the reduced scale. Here, the scale of the numerical analysis is reduced to one-fifth. The distribution patterns of the numerical analysis are similar to those of the experimental results, except for the position of the maximum pressure on the z-axis. In the case of the water tank experiment, the image points, which are the maximum pressure points, are located far from the lens compared with those of the numerical analysis, as shown in Fig. 4. This is caused by the sound source condition of the 3-D FDTD method, that is, the planar source. Similar trends, in which the focal point of the spherical source is far from the lens compared

with that of the planar source, were calculated in our previous research [4, 5]. Whenever the incidence angle increases by 1 deg, the image point shifts to the right by about 10 mm.

The -3 dB area, whose pressure is 3 dB lower than the maximum at the image point, is used for evaluating the directional resolution of the lens, the same as the 3 dB beam width. The -3 dB areas on the x-z plane are shown in Fig. 5. The shapes of the -3 dB areas in the experimental results are similar to those in the analysis results. We can also see that each -3 dB area has a width of about 8 mm and that the -3 dB areas do not overlap. Thus we verified that a sufficient resolution for the ANI system can be realized using a lens with an aperture diameter of 2.0 m at small incidence angles.

4.2 Frequency dependence

The on-axis characteristics and beam patterns of experimental results are compared with those of the numerical analysis at normal incidence in Figs. 6 and 7, respectively. Here, the scale of the numerical analysis is reduced to one-fifth again. The shapes of the on-axis characteristics of the numerical analysis in Fig. 6(a) are similar to those of the experimental results in Fig. 6(b). However, the on-axis peaks of the analysis results are forward-biased compared with those of the experimental results. This is also caused by the sound source condition described above. The peaks remain at 200, 300, and 500 kHz in Fig. 6(b). However, that at 100 kHz is forward biased compared with those of other frequencies. The difference between the peak pressure level and the level on the peak position at other frequencies is very small, because the distribution is broad at 100 kHz. In this case, the frequency dependence of the peak position on a low frequency is ignored although the reason is not clear. The shapes of the main-lobes of four beam patterns of the experimental results are similar to those of numerical analysis, as shown in Figs. 7(a)-(d). However, the side-lobe level of the experimental result is slightly larger than that of the numerical analysis. We consider these errors to be small enough to be acceptable, since they do not affect to estimate -3 dB areas. The beam patterns are expanded and constructed in proportion to the wave length. It is likely that the -3 dB areas will not overlap over 300 kHz, because the main-lobe at 500 kHz is narrower than that at 300 kHz.

5 Conclusion

In this study, to confirm the directional resolution of a tested lens in a wide frequency band of 20-100 kHz, we performed a reduced scale experiment of one-fifth space in a water tank. The results showed that the sound pressure distributions of the experiment and numerical analysis are in good agreement. In addition, the main-lobe at 500 kHz was narrower than that at 300 kHz in the beam pattern of the reduced scale. This suggests that the lens of 2.0 m aperture will have fine directional resolution over 60 kHz in the original scale. Future studies are still needed to measure the sound pressure field at oblique incidences. Tests are needed to confirm that -3 dB areas do not overlap each other at different angle of incidence over 300 kHz.

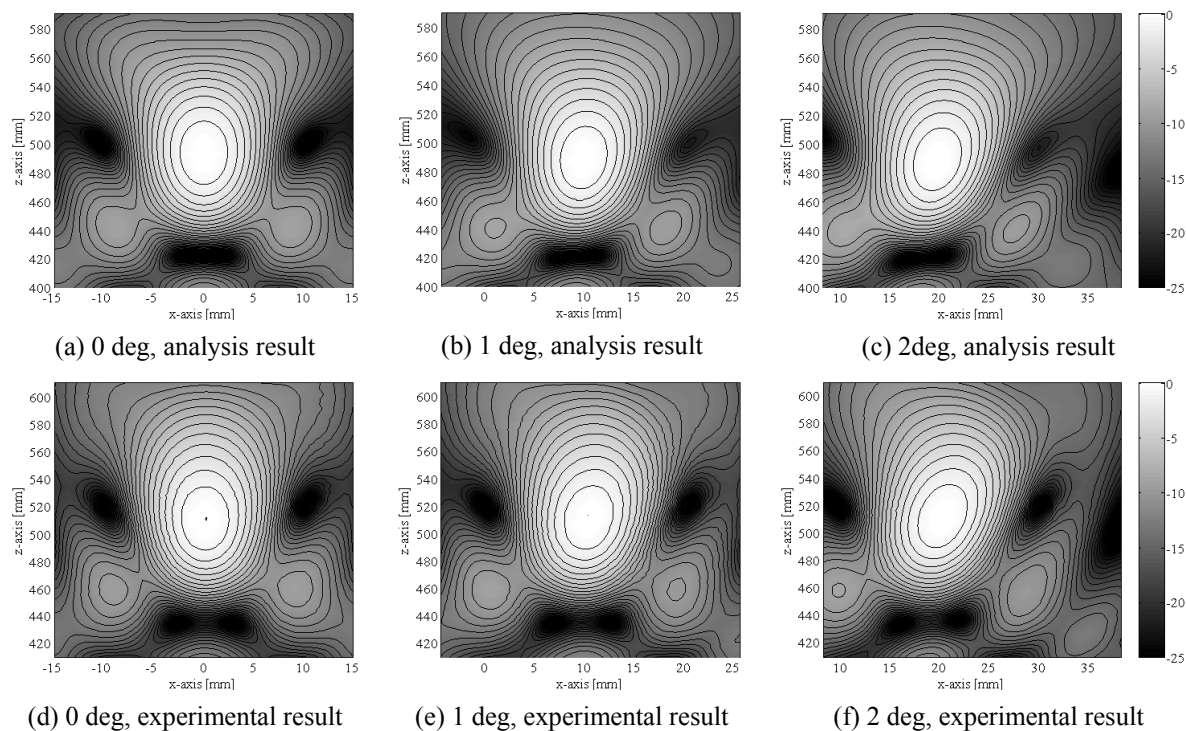


Fig. 4 Sound pressure distributions on the x-z plane at y=0 are compared between the numerical analysis and experimental results. The numerical analysis results are at 0 deg in (a), at 1 deg in (b), and at 2 deg in (c). The experimental results are at 0deg in (d), at 1 deg in (e), and at 3 deg in (f). The frequency is 300 kHz, which is the target center frequency on the reduced scale.

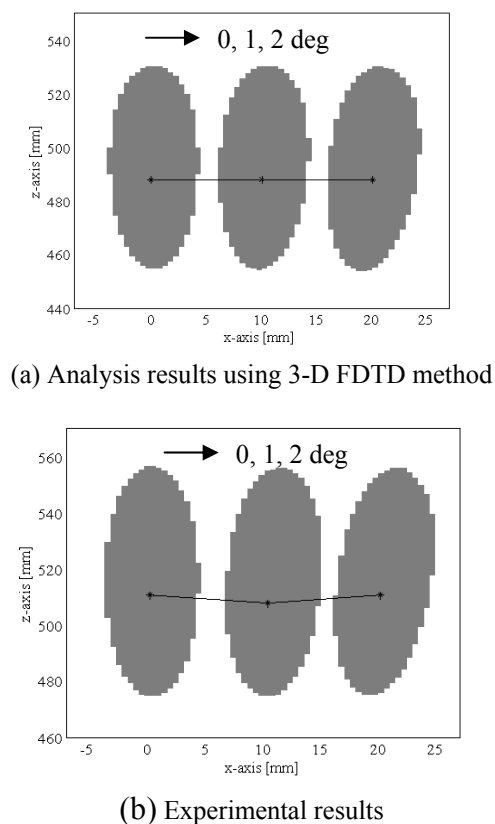


Fig. 5 The -3 dB areas of the x-z plane at y=0 are compared between the numerical analysis and experimental results. The numerical analysis results are in (a), and the experimental results are in (b). The frequency is 300 kHz, which is the target center frequency on the reduced scale.

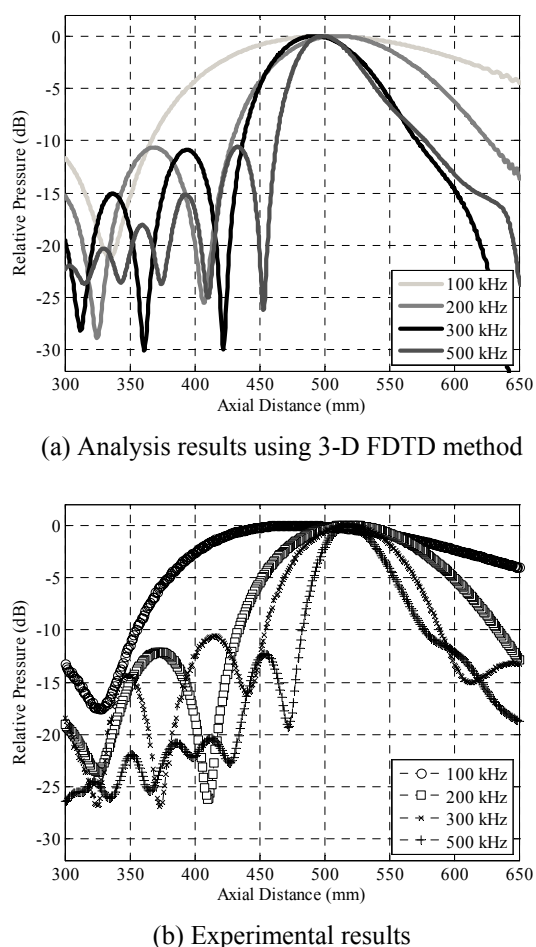
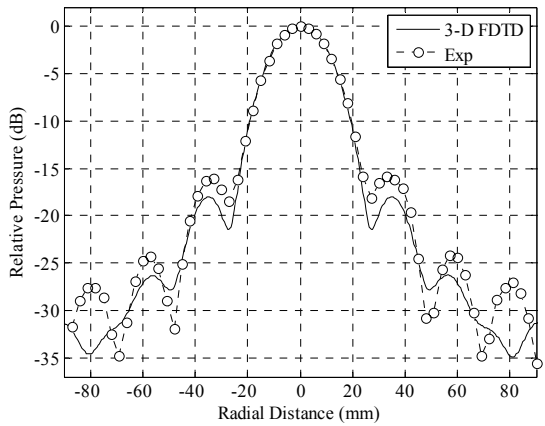
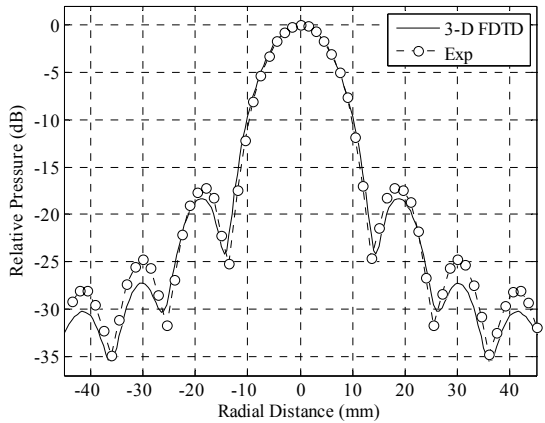


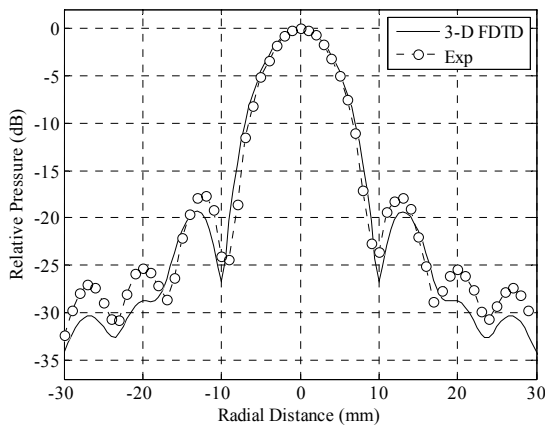
Fig.6 Comparison of on-axis characteristics at various frequencies.



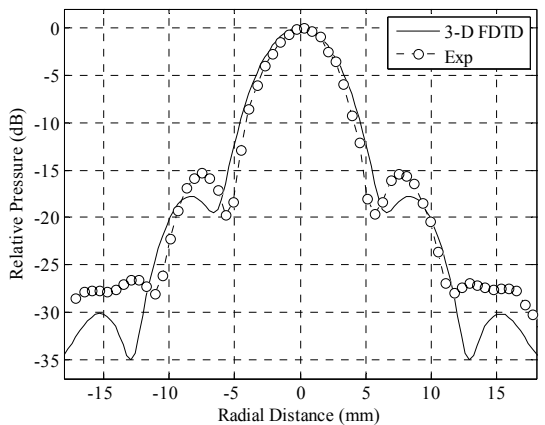
(a) 100 kHz



(b) 200 kHz



(c) 300 kHz



(d) 500 kHz

Fig. 7 Comparison of beam patterns at various frequencies.

References

- [1] M. J. Buckingham, B. V. Verkhout, S. A. L. Glegg, "Imaging the Ocean with Ambient Noise", *Nature* 356, 327-329 (1992)
- [2] C. L. Epifanio, J. R. Potter, G. B. Deane, M. L. Readhead, M. J. Buckingham, "Imaging in the Ocean with Ambient Noise: the ORB Experiments", *J. Acoust. Soc. Am.* 106, 3211-3225 (1999)
- [3] P. Venugopalan, M. A. Chitre, E. T. Tan, J. Potter, K. T. Beng, S. B. Ruiz, S. P. Tan, "Ambient Noise Imaging – First Deployments of ROMANIS and Preliminary Data Analysis", *Proc. Oceans 2003 Marine Technology and Ocean Science Conf.*, CD-ROM (2003)
- [4] K. Mori, A. Miyazaki, H. Ogasawara, T. Yokoyama, T. Nakamura, "Finite Difference Time Domain Analysis of Underwater Acoustic Lens System for Ambient Noise Imaging", *Jpn. J. Appl. Phys.* 45, 4834-4841 (2006)
- [5] K. Mori, A. Miyazaki, H. Ogasawara, T. Yokoyama, T. Nakamura, "Numerical Analysis of an Underwater Acoustic Lens System for Ambient Noise Imaging using Finite Difference Time Domain Method", *Proc. IEEE OCEANS '06 ASIA PACIFIC Conf.*, CD-ROM (2006)
- [6] K. Mori, H. Ogasawara, T. Nakamura, "Reduced Scale Experiment of Single Spherical Biconcave Acoustic Lens System for Ambient Noise Imaging" *Proc. 2nd Int. Conf. Underwater Acoustic Measurements: Technologies and Results* CD-ROM (2007)
- [7] K. Mori, H. Ogasawara, T. Nakamura, "Small-Scale Trial for Evaluating Directional Resolution of Single Spherical Biconcave Acoustic Lens in Designing of Ambient Noise Imaging System" *Jpn. J. Appl. Phys.* 39 (2008) [to be published]
- [8] W. W. L. Au, K. Banks, "The Acoustics of the Snapping Shrimp *Synalpheus parneomeris* in Kaneohe Bay", *J. Acoust. Soc. Am.* 103, 41-47 (1998)
- [9] F. Iijima, T. Tsuchiya, N. Endoh, "Analysis of Characteristics of Underwater Sound Propagation in the Ocean by a Finite Difference Time Domain Method", *Jpn. J. Appl. Phys.* 39, 3200-3204 (2000)
- [10] Y. Yamada, S. Maeda, T. Tsuchiya, N. Endoh, "Analysis of Sound Field of Aerial Ultrasonic Sensor by Three-Dimensional Finite-Difference Time-Domain Method Using Parallel Computing", *Jpn. J. Appl. Phys.* 43, 2869-2870 (2004)
- [11] K. Mori, T. Nakamura, T. Yokoyama, A. Hasegawa, "3-D FDTD Analysis of Sound Field Focused by Biconcave Acoustic Lens for Normal Incidence", *Jpn. J. Appl. Phys.* 44, 4696-4701 (2005)